Supporting Information

Effects of Bile Salt Sodium Glycodeoxycholate on the Self-Assembly of PEO-PPO-PEO Triblock Copolymer P123 in Aqueous Solution

Solmaz Bayati,[1] Luciano Galantini,[2] Kenneth D. Knudsen,[3] and Karin Schillén[1,]*

[1] Division of Physical Chemistry, Department of Chemistry, Lund University, P.O. Box 124, SE-221 00 Lund, Sweden

[2] Department of Chemistry, "Sapienza" University of Rome, P. le A. Moro 5, 00185 Rome, Italy

[3] Institute for Energy Technology, P.O. Box 40, NO-2027 Kjeller, Norway

Corresponding Author. *E-mail: Karin.Schillen@fkem1.lu.se

RESULTS AND DISCUSSION

DSC Results. DSC measurements were performed on mixed P123-NaGDC solutions at different NaGDC/P123 molar ratios, in addition to pure solutions of P123 and NaGDC. The thermograms, expressed as apparent molar heat capacity of the sample, C_p^{app} vs temperature,[1] display one main transition peak characterized by an onset temperature, T_{onset}, and a peak maximum temperature, T_m. T_{onset} was calculated from the intersection point of the linear extrapolation of the baseline and the peak ascent. The area under the peak gives the enthalpy of transition, ΔH_{tr}. The peak width at half height, $\Delta T_{1/2}$, was evaluated as well. The curve of the pure P123 solution also presented a small endothermic peak related to the sphere-to-rod transition of the micelles with a peak maximum at T_m(sphere-to-rod) = 61.9 °C, which is in a good agreement with ref 2. The results are presented in Figure 1 in the article and in Table S1, below.

Table S1. Onset temperature T_{onset}, temperature of peak maximum T_m, enthalpy of transition ΔH_{tr}, peak width at half height $\Delta T_{1/2}$, and ratio between $\Delta T_{1/2}$ and ΔH_{tr} for P123 in water and for aqueous mixed P123-NaGDC solutions at different molar ratios, MR.

C_{NaGDC} (mM)	C_{P123} (mM)	MR[1]	T_{onset} (°C)	T_m (°C)	$\Delta T_{1/2}$ (°C)	ΔH_{tr} (kJ mol^{-1})	$\Delta T_{1/2}$ / ΔH_{tr} (°C mol kJ^{-1})
0	1.74	0	17.6	20.7	4.5	426	0.011
1.02	1.74	0.6	17.6	20.2	4.2	420	0.010
5.14	1.74	3.0	17.8	19.3	3.7	336	0.011
9.80	1.74	5.6	19.5	20.4	4.6	270	0.017
21.5	1.74	12	21.5	23.6	6.1	171	0.036
38.9	1.73	22	24.1	25.8	6.2	102	0.061
57.5	1.74	33	25.7	27.8	6.3	78	0.081
87.1	1.73	50	27.7	29.9	6.4	50	0.129
95.2	1.74	55	28.5	30.5	6.0	41	0.146
200	1.72	116	32.2	34.8[2]	6.6	18[2]	0.368[2]
250	1.73	144	32.9	35.1[2]	3.6	4.5[2]	0.810[2]

[1] MR $= n_{\mathrm{NaGDC}}/n_{\mathrm{P123}}$, where n_{NaGDC} is the number of moles of NaGDC and n_{P123} is the number of moles of NaGDC. [2] Value with high uncertainty.

The DSC curve of the pure P123/water system presented in this work shows an endothermic signal, which is related to the temperature-induced micellization of P123 (Figure 1 in the article). The peak is broad but still well-defined in terms of onset- and maximum temperatures, see, e.g., ref 3. Due to the gradual decrease in solubility of PPO and because of that these polymers are inherently polydisperse and impure, the transition takes place within certain temperature range.[4-10] This is referred to in the literature as the *unimer-to-micelle transition regime* – a temperature-regime where both unimers and micelles coexist.[2] Our group has previously studied the concentration dependence on CMT of some PEO-PPO-PEO copolymers including P123.[11]

A mass-action model has been developed to fit the calorimetric output of the temperature dependent micellization process in aqueous PEO-PPO-PEO block copolymer systems.[9, 12, 13] From the model-fitting estimates for the aggregation number and the thermodynamic parameter, the van't Hoff enthalpy (ΔH_{vH}) was obtained. ΔH_{vH} characterizes the temperature dependence of the change in equilibrium composition of unimers and micelles and it is related to the transition width, see, e.g., ref 9. The gradual micellization of PEO-PPO-PEO copolymers arises because of the small values of ΔH_{vH}. The ratio of the van't Hoff enthalpy to the measured calorimetric enthalpy ($\Delta H_{vH}/\Delta H_{tr}$) provides a measure of the cooperativity of the transition, i.e., the ratio is a reflection of the number of molecules that cooperate in the transition. When ΔH_{vH} increases, the width of the transition becomes increasingly smaller, indicative for a process of high cooperativity. However, for systems with a temperature dependent self-assembly behavior, the van't Hoff equation does not always lead to reliable results.[14] Recently, a new model for describing DSC experiments on PEO-PPO-PEO block copolymers in water has been published.[15] The presented model, which also is based on a mass-action model, considers the temperature dependence of the aggregation number of the copolymer micelles. It was shown that by using

this model a quantitative description of the DSC thermograms could be made without any discrepancy between ΔH_{vH} and ΔH_{tr}.

Based on this information, qualitative conclusions about the relation between the peak shape and cooperativity in the mixed P123-NaGDC system could be made. In this work, an endothermic signal was obtained also for the mixed P123-NaGDC solutions with low contents of NaGDC, which then indicated that complexes with a dehydrated PPO core were formed at those conditions. We noted that the cooperativity of complex formation was similar to that of the P123 micellization at low NaGDC concentration and that the cooperativity decreased, i.e., the peak broadened and decreased in amplitude, with increasing amount of bile salt in the mixture. This indicates that the solution contained fewer P123 micelle-NaGDC complexes and/or complexes with lower aggregation numbers. Finally the peak vanished at high bile salt concentrations, i.e., the cooperativity was lost, which led to the conclusion that no large P123-bile salt micellar complexes were present in those mixtures (Figure 1). In Table S1, we have listed the ratio of the peak width at half height ($\Delta T_{1/2}$) and the transition enthalpy, $\Delta T_{1/2}/\Delta H_{tr}$ as a measure of the cooperativity of the self-assembly process.

For the mixed P123-NaGDC solutions at higher MR (12 – 116), the measured DSC traces demonstrated a broad endothermic peak at temperatures below the onset of the main peak, see Figure S1, where the results for MR = 33 – 116 are presented.

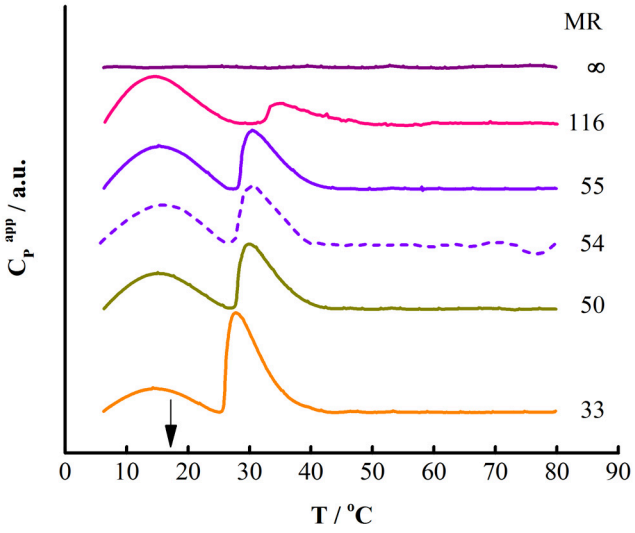

Figure S1. DSC curves of mixed P123-NaGDC solutions containing 1.74 mM P123 and with various NaGDC/P123 molar ratios in the high molar ratio regime (same data as in Figure 1 in the article). Also shown is the curve of a 95.8 mM NaGDC solution (MR = ∞, purple line). The arrow marks T_{onset} of MR = 0. The scan rate was 1 °C/min. The DSC curve of MR = 54 from an experiment performed at 0.2 °C/min is shown as a dashed line.

A similar phenomenon has recently been observed in DSC experiments performed on mixed solutions of PEO-PPO-PEO block copolymers and ammonium gemini surfactants.[16] In that study, this peak was interpreted as being related to the formation of small surfactant-copolymer complexes where surfactant micelles bind to the unassociated copolymer unimers. Based on their conclusion, our results thus indicated that small "NaGDC-P123" complexes (rich in GDC^- anions), pictured as NaGDC micelles with one or several P123 unimers included, were formed before the onset of the main transition peak. Another observation was that the maximum of the peak did not differ significantly in temperature upon increasing the NaGDC. This further strengthens the argument that the signal was related to a process in which copolymer chains

associated with bile salt micelles that already exist in the solutions at high molar ratios of NaGDC. A measurement at a lower scan rate (0.2 °C/min) of the mixed solution at MR = 54 gave a similar trace as that of MR = 55 measured at scan rate 1 °C/min and we could thus rule out that the pre-peak was an artifact due to a high scan rate.

Model for NaGDC-P123 Complex Formation Based on DSC Data. We proposed that the suppression of the P123 self-assembly is related to the formation of complexes between P123 unimers and NaGDC micelles. At temperatures below the critical micelle temperature of P123 (<17.6 °C) and at bile salt concentrations above the critical micelle concentration (CMC) of NaGDC, a fraction of P123 is partly dehydrated because of the interaction with NaGDC and therefore do not contribute to the signal of the main transition peak in the DSC thermograms. If we consider that the free hydrated unimers at CMC remain after cooperative aggregation and the fraction (relative to the total concentration of P123) of complexed P123 unimers in solution is defined as f, then we can write the following equations with the same proportionality constant

$$\Delta H_{tr,0} \propto ([P]_{tot} - \mathrm{CMC(P123)}) \quad \text{(S1)}$$

$$\Delta H_{tr} \propto ([P]_{tot} - \mathrm{CMC(P123)} - f[P]_{tot}) \quad \text{(S2)}$$

where $\Delta H_{tr,0}$ and ΔH_{tr} are the enthalpies of transition for the pure P123 solution and the P123-NaGDC mixed solution, respectively, $[P]_{tot}$ is the total P123 concentration and CMC(P123) is the temperature-dependent critical micelle concentration of P123, taken at the T_{onset} value of the transition corresponding to each molar ratio (the CMC values were deduced from interpolation of the data in the work of Alexandridis et al.[17]).

By combining Eq S1 and Eq S2, the following ratio is obtained

$$\frac{|\Delta H_{tr}-\Delta H_{tr,0}|}{\Delta H_{tr,0}} = \frac{f}{\left(1-\frac{\mathrm{CMC(P123)}}{[P]_{tot}}\right)} \quad \text{(S3)}$$

which can be rearranged to

$$f = \frac{|\Delta H_{tr}-\Delta H_{tr,0}|}{\Delta H_{tr,0}} \cdot \left(1-\frac{\mathrm{CMC(P123)}}{[P]_{tot}}\right) \quad \text{(S4)}$$

which in turn is reported in the article and plotted in Figure 2 in the article.

Let us assume that only one P123 unimer is included in one NaGDC micelle according to the equilibrium

$$S_n + P \leftrightharpoons S_nP \quad \text{(S5)}$$

where S_n is the bile salt micelle with aggregation number n, P and S_nP denote the block copolymer chain and the NaGDC micelle carrying one P123 unimer (i.e., the NaGDC-rich complex), respectively.

Based on the process for the complex formation given in Eq S5, the above-defined fraction of complexed P123 unimers f is given by

$$f = \frac{[S_nP]}{[P]_{tot}} \quad \text{(S6)}$$

where the brackets denote molar concentrations.

The equilibrium constant for the complex formation is

$$K = \frac{[S_nP]}{[S_n][P]} = \frac{f}{[S_n](1-f)} \quad \text{(S7)}$$

Furthermore, the total NaDGC concentration $[S]_{tot}$ is a sum of the NaGDC molecules that are free in solution and those in the NaGDC micelles

$$[S]_{tot} = \text{CMC(NaGDC)} + n[S_n] \quad \text{(S8)}$$

Finally, the combination of Eq S7 and Eq S8 gives the model equation used to fit of the DSC data presented in Figure 2 in the article

$$f = \frac{\frac{\text{K}}{n}[[S]_{tot} - \text{CMC(NaGDC)}]}{1 + \frac{\text{K}}{n}[[S]_{tot} - \text{CMC(NaGDC)}]} \quad \text{(S9)}$$

It has been shown by Yu et al. that the enthalpy of micelle formation of PEO-PPO-PEO block copolymers ($\Delta H_{tr,0}$) can be derived from the variation of the critical micelle temperature (CMT) with copolymer concentration c [5]

$$\Delta H_{tr,0} = R[d \ln c / d(1/\text{CMT})] \quad \text{(S10)}$$

The expression in Eq S10 was employed in a systematic fluorescence spectroscopy study on the micellization of PEO-PPO-PEO block copolymers in water [17] and also in our previous DSC study on the micelle formation of P123.[11] Eq S10 demonstrates (under the assumption that $\Delta H_{tr,0}$ is constant within the investigated CMT range), that there is a linear dependence between $\ln c$ and 1/CMT. Using the data of Alexandridis et al.,[17] the linear equation presented above in Eq S10 can be retrieved, which in turn can be used to interpolate the $\ln c$ values from the CMT (i.e., T_{onset}) values measured for the mixed P123-NaGDC solutions investigated in this work (see Table S1). These concentrations correspond to the concentration of free P123 unimers $[\text{P123}]_{free}$, which vary with the bile salt concentration because of the complex formation with the bile salt micelles, i.e., small NaGDC-rich complexes. The fraction of complexed unimers can

be obtained from the estimated fraction of free P123 unimers f_{free} (= $[\mathrm{P123}]_{free}$ /$[\mathrm{P123}]_{tot}$, where $[\mathrm{P123}]_{tot}$ is the total P123 concentration): $f_{complexed} = 1 - f_{free}$.

In Figure S2, $f_{complexed}$ (estimated from the CMT's as described above) is presented as a function of NaGDC concentration together with that obtained from the reported ΔH_{tr} values, f, and fitted to the model presented above.

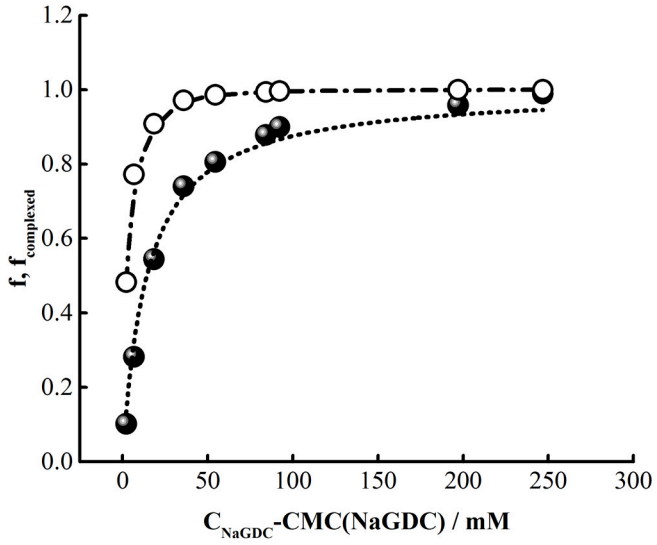

Figure S2. The fraction of complexed P123 unimers f obtained from measured ΔH_{tr} (filled symbols) and the fraction of complexed P123 unimers $f_{complexed}$ estimated from the CMT (i.e., T_{onset}) values (open symbols), as a function of NaGDC concentration C_{NaGDC} corrected for CMC of NaGDC (3 mM) in mixed P123-NaGDC solutions containing 1.74 mM P123. The dotted line is the model fit (Eq S9), and the dash-dotted line is a guide to the eye.

Both data sets show a similar trend (the $f_{complexed}$-curve being more steep), however, they do not coincide. This is not in contrast with the proposed model since the relation between the CMT and the concentration c presented above is based on thermodynamical analysis of a pure self-

assembling system but it is not valid for a system that contains free unimers and unimers included in NaGDC micelles. It is important to clarify that we do not propose that it is only the free unimers that self-assemble at the CMT. But, they are the ones that contribute to the measured ΔH_{tr} due to dehydration, although the transition is complex and involves all species in the system (both NaGDC micelles with included unimers and free unimers). Those complexed with bile salt micelles do not contribute to the signal since they are already partly dehydrated (recall that the signal is related to the dehydration of the PPO blocks). However, the complexed unimers may still be involved in the *formation* of the P123 micelle-NaGDC complexes (without being rehydrated prior to it). As the amount of added bile salt increases, fewer free unimers are available thus causing the DSC signal to decrease.

DLS Results. The temperature dependence of a mixed solution in the high concentration regime containing 1.74 mM P123 and 95.8 mM NaGDC (MR = 55) was investigated by DLS. Figure S3 shows the results in the form of relaxation time distributions $\tau A(\tau)$ vs. $\log(\tau/\mu s)$ at different temperatures ranging from 20 to 60 °C and at θ = 90°.

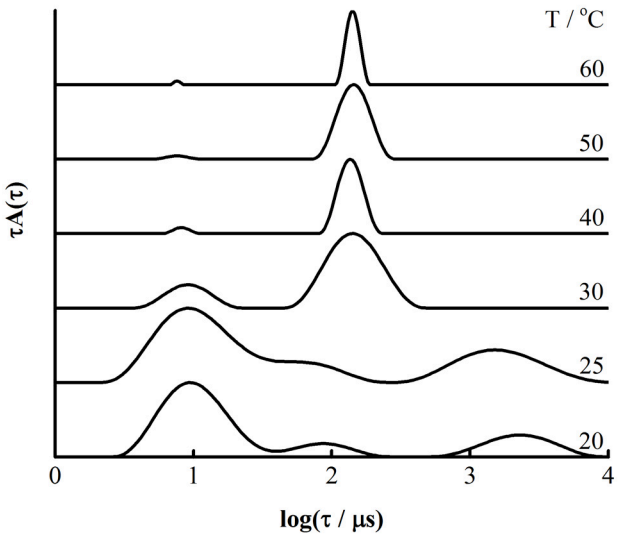

Figure S3. Relaxation time distributions for a 1.74 mM P123 solution with 95.8 mM NaGDC (MR = 55) at the indicated temperatures. Measurements at $\theta = 90°$. The data have been shifted by a factor (T/η_0) on the $\log(\tau/\mu s)$ -axis and normalized by height.

At the lowest temperatures (20 and 25 °C), the distributions exhibited a quite complicated multimodal behavior with several broad peaks, which in turn reflected the fact that it was difficult to obtain satisfying intensity correlation functions because of the low scattering intensity under these conditions. The fast mode with the highest amplitude was attributed to the NaGDC-P123 complexes, whereas the slowest mode was related to the clusters of the pure P123 system (Figure 3a in the article). The unresolved middle peak may be an indication of the system being on the verge of forming P123 micelle-NaGDC complexes. This result was in agreement with that from the DSC measurement performed on a solution in which a molar ratio close to this solution (MR = 55) gave a CMT value of 27.8 °C (Table S1). At 30 °C (close to the T_m for MR = 55), only two relaxation modes were observed; the slow one corresponded to P123 micelle-NaGDC complexes and the fast one, as before, to the NaGDC-P123 complexes. At higher temperatures,

the distributions remained unchanged in consistency with the DSC data. The system did not pass through any other aggregation process at these temperatures.

EXPERIMENTAL SECTION

Differential Scanning Calorimetry. High sensitivity differential scanning calorimetry was used to determine the transition enthalpies and transition temperatures of 1.74 mM (= 1.00 wt %) P123 solutions with varying bile salt concentration. The measurements were performed using a VP-DSC high-sensitivity differential calorimeter (MicroCal, Inc., Northampton, MA, USA). The volume of both the sample and reference cells was 0.5065 mL. Water was used as a reference in all measurements. For all sample solutions, two consecutive up-scans were carried out in the temperature range 5 – 80 °C with a scanning rate of 1 °C/min. The cold solution was injected into the sample cell to be equilibrated at 5 °C for 20 minutes before the scan was started. After the first scan, the temperature was decreased and the sample was again left to equilibrate at 5 °C for 20 minutes before the second scan was performed. For all of the samples, the result of the second scan was identical to that of the first, hence only first scans are presented in this work. The instrument measures the difference in heat capacities of an equal volume of the sample and the reference versus temperature at a constant pressure, and the signal is proportional to the apparent molar heat capacity of the sample, C_p^{app}.[1] The enthalpy of transition (here alternatively association) ΔH_{tr} is obtained by integration of the peak in the received thermogram, where C_p^{app} is plotted against the temperature. The onset temperature of the transition, T_{onset}, is calculated from the intersection point of the linear extrapolation of the baseline and the peak ascent. The temperature at which the peak has a maximum is called the transition temperature, T_m, and the

peak width at half height is denoted $\Delta T_{1/2}$. The Origin software was used for data analysis. The assessed values are presented in Table S1, above.

Dynamic and Static Light Scattering. Dynamic and static light scattering measurements were carried out by means of an ALV/DLS/SLS-5022F, CGF-8F-based compact goniometer (ALV-GmbH, Langen, Germany). A 22 mW He-Ne laser with the wavelength of 632.8 nm was used as the light source. The intensity of the incident light was controlled by means of a software-commanded attenuator. A perfect vertical polarization was achieved using a Glan laser polarizer prism with a polarization ratio better than 10^5 in front of the high-temperature cell housing. The cell housing was composed of a thermostated cylindrical quartz container, which was filled with a refractive index-matched liquid (*cis*-decahydronaphtalene). The detection unit, composed of a near-monomodal optical fiber and two high-quality avalanche photodiodes placed in the pseudo-cross geometry, was responsible for collecting the unpolarized scattered light used for generating pseudo-cross correlation functions. An F32 Julabo heating circulator was used to control the temperature (± 0.01 ºC). A more detailed description of the instrument can be found in ref [18]. The DLS and the SLS experiments were performed in the temperature range of 15 – 60 °C. The solutions were filtered cold into 10-mm clean cylindrical borosilicate glass cells through a sterile 0.20 μm Minisart© filter (Sartorius, Germany) and were equilibrated at the measuring temperature for 30 minutes, prior to the measurement. For measuring temperatures above room temperature, the solutions were equilibrated for at least 60 minutes at room temperature and thereafter at the measuring temperature for 30 minutes to avoid kinetic effects caused by fast temperature changes over the critical micellization temperature.[19]

The DLS measurements were performed at six different scattering angles, θ, in the range from 40° to 130°. The SLS experiments were carried out by first measuring the angular dependence of the time-average of the intensity of scattered light, $I_s(\theta)$. No angular dependence, which is indicative for a system of small scattering particles, was found for any of the solutions. As a consequence the measurements were performed at θ = 90°. The scattering from the solvent was not subtracted. The intensity is expressed in terms of the total Rayleigh ratio defined as

$$R_\theta = (I_s(\theta)/I_0)R_{tol}(n/n_{tol})^2 \quad \text{(S11)}$$

where I_0 is the incident laser intensity, R_{tol} is the literature value of the Rayleigh ratio of toluene at 90° (R_{tol} = 1.4206 · 10^{-5} cm^{-1}) and $(n/n_{tol})^2$ is the Herman-Levinson correction factor of the scattering volume where n_{tol} = 1.496 is the refractive index of toluene.

DLS Data Analysis. In a DLS experiment, the time correlation function of the scattered intensity, $G^{(2)}(t)$ is measured (in pseudo-cross-correlation mode in this work) and the normalized form, $g^{(2)}(t)$, is obtained directly from the software of the correlator during the measurement presented with $g^{(2)}(t) - 1$ as *y*-values. The normalized time correlation function of the electric field, $g^{(1)}(t)$, is related to $g^{(2)}(t)$ through Siegert's equation[20]

$$g^{(2)}(t) - 1 = \beta\left|g^{(1)}(t)\right|^2 \quad \text{(S12)}$$

where t is the lag time and β ($\leq$ 1) is the coherence factor that considers the deviations from ideal correlation.

For a particle system, which is monodisperse in size, $g^{(1)}(t)$ is a single-exponential function. However, for a polydisperse system the function is multiexponential. To obtain the relaxation

time distribution, $A(\tau)$, in the latter system, an inverse Laplace transformation of $g^{(1)}(t)$ is usually required

$$g^{(1)}(t) = \int_{-\infty}^{\infty} \tau A(\tau) \exp(-t/\tau)\, d\, ln\tau \quad \text{(S13)}$$

where $\tau = 1/\Gamma$, is the relaxation time and Γ is the relaxation rate or frequency. Γ is obtained from the first moment of the corresponding mode in the relaxation time distribution.

A constrained nonlinear inverse Laplace transformation regularization algorithm REPES (Regularized Positive Exponential Sum), which fits with respect to the measured $g^{(2)}(t)$ directly, was used in the data fitting procedure.[20, 21] The regularizing term is adjustable and a value of 0.5 was chosen as standard in all the analyses presented in this work. The analyzed relaxation time distributions are here presented as $\tau A(\tau)$ vs. $\log(\tau/\mu s)$ for an area equal to 1 representation.

The collective translational diffusion coefficient D of scattering particles in solution at a finite concentration (i.e., with interparticle interactions present) is defined in the limit of small scattering vectors as

$$D = \lim_{q \to 0}(\Gamma/q^2) \quad \text{(S14)}$$

where $q = 4\pi n \sin(\theta/2)/\lambda$ is the magnitude of the scattering vector, n is the refractive index of the medium, which for dilute solutions, as in this case, can be taken to be the refractive index of water, θ is the scattering angle and λ is the wavelength of the incident light.

From DLS measurements at different scattering angles, D is thus evaluated from the slope of Γ as a function of q^2. In this study, all relaxation rates were found to be q^2 dependent (with a zero

intercept) and thus corresponded to a translational diffusive motion. The apparent hydrodynamic radius can thereafter be estimated using the Stokes-Einstein equation

$$R_{H,app} = kT/6\pi\eta_0 D \quad \text{(S15)}$$

where k is the Boltzmann constant, η_0 is the viscosity of the solvent (here water) at the absolute temperature T.

Electrophoretic Mobility. A Zetasizer Nano ZS (Malvern Instruments Ltd., Worcestershire, UK) was used for the electrophoretic mobility experiments. The instrument operated with a 4 mW He-Ne laser as a light source. The sample was placed in a disposable folded capillary cell, DTS1070 (Malvern Instruments Ltd., Worcestershire, UK) and the scattered light was detected at a scattering angle of 17°. More information on the instrument can be found in ref [18]. The electrophoretic mobility, u_e of a charged particle in solution can be calculated from its velocity, $\overline{V}$ which is measured after applying an electric field $\overline{E}$[18]

$$u_e = \overline{V}/\overline{E} \quad \text{(S16)}$$

All measurements of u_e were performed at 40 °C. Prior to the measurements, the solutions were equilibrated at room temperature for one hour and thereafter at 40 °C for 30 minutes (see explanation above, under the light scattering section). The reported u_e value is an average of three subsequent measurements. The errors are given ± standard deviation (sd).

Small Angle X-Ray Scattering. Small angle X-ray scattering (SAXS) measurements were performed at MAX II SAXS beamline I911-4 at the MAXIV Laboratory in Lund, Sweden.[22] The X-ray scattering intensity was recorded at wavelength λ = 0.91 Å on a 165-mm-diameter MarCCD detector, which was placed at a sample-to-detector distance (2.311m) corresponding to

a q range of 0.0057 – 0.4 Å^{-1} that was calibrated using silver behenate as a standard. The two-dimensional (2D) SAXS patterns were processed using Fit2D software.[23] The temperature was kept at 50 ± 0.5 °C using with an external heating circulator. The integrated scattering functions of the samples were corrected for scattering contributions of the capillary and the solvent (water) and thereafter put on an absolute scale using water as a calibration standard.[24]

SAXS Data Analysis. The scattering intensity of a solution of n interacting monodisperse spherical particles per volume is dependent on the structure of the particles and the interparticle interactions according to[25]

$$I(q) \propto nP(q)S(q) \tag{S17}$$

where the two contributions are accounted for by the form factor $P(q)$ (intraparticle effects) and by the structure factor $S(q)$ (interparticle effects).

An indirect Fourier transformation method was recently developed by Hansen that allows for the separation of the two effects using an excluded volume distribution to describe the interparticle interactions.[26] With this method a structure factor, without a priori information of the specific details of the interparticle interaction, as well as information on the particle size, shape and internal structure in terms of the distance distribution function, $p(r)$, as usually obtained in IFT methods, can be extracted simultaneously (r is the distance between pairs of scattering material within the particle). The $p(r)$ function can be integrated to obtain the particle gyration radius and it is expected to vanish at the particle maximum distance, D_{max}. The scattering intensity is linked to $p(r)$ by the following Fourier integral

$$I(q) = 4\pi \int_0^\infty p(r) \frac{\sin qr}{qr} dr \tag{S18}$$

We have employed this data analysis method to interpret SAXS data of pure block copolymer micelles in 8.68 P123 solution (= 5.00 wt% P123) and of charged P123 micelle-NaGDC complexes at NaGDC/P123 molar ratio, MR = 0.3 (2.72 mM NaGDC) and MR = 0.6 (5.21 mM NaGDC). The experimental data are presented together with the curves from the fits in Figure 7a in the article with the analyzed structure factors shown in the inset.

REFERENCES

(1) Olofsson, G.; Wang, G., Isothermal Titration and Temperature Scanning Calorimetric Studies of Polymer-Surfactant Systems. In *Polymer–Surfactant Systems*, Kwak, J. C. T., Ed. Marcel Dekker: New York, 1998; pp 317-356.

(2) Löf, D.; Niemiec, A.; Schillén, K.; Loh, W.; Olofsson, G., A Calorimetry and Light Scattering Study of the Formation and Shape Transition of Mixed Micelles of $EO_{20}PO_{68}EO_{20}$ Triblock Copolymer (P123) and Nonionic Surfactant ($C_{12}EO_6$). *J. Phys. Chem. B* **2007,** *111*, 5911-5920.

(3) Wanka, G.; Hoffman, H.; Ulbricht, W., Phase Diagrams and Aggregation Behavior of Poly(oxyethylene)-Poly(oxypropylene)-Poly(oxyethylene) Triblock Copolymers in Aqueous Solutions. *Macromolecules* **1994,** *27*, 4145-4159.

(4) Brown, W.; Schillén, K.; Almgren, M.; Hvidt, S.; Bahadur, P., Micelle and Gel Formation in a Poly(ethylene oxide)-Poly(propylene oxide)-Poly(ethylene oxide) Triblock Copolymer in Water Solution. Dynamic and Static Light Scattering and Oscillatory Shear Measurements. *J. Phys. Chem.* **1991,** *95*, 1850-1858.

(5) Yu, G.-E.; Deng, Y.; Dalton, S.; Wang, Q.-G.; Attwood, D.; Price, C.; Booth, C., Micellisation and Gelation of Triblock Copoly(oxyethylene/oxypropylene/oxyethylene), F127. *J. Chem. Soc. Faraday Trans.* **1992,** *88*, 2537-2544.

(6) Glatter, O.; Scherf, G.; Schillén, K.; Brown, W., Characterization of a Poly(ethylene oxide)-Poly(propylene oxide) Triblock Copolymer (EO_{27}-PO_{39}-EO_{27}) in Aqueous Solution. *Macromolecules* **1994,** *27*, 6046-6054.

(7) Batsberg, W.; Ndoni, S.; Trandum, C.; Hvidt, S., Effects of Poloxamer Inhomogeneities on Micellization in Water. *Macromolecules* **2004,** *37*, 2965-2971.

(8) Linse, P., Micellization of Poly(ethylene oxide)-Poly(propylene oxide) Block Copolymers in Aqueous Solution: Effect of Polymer Polydispersity. *Macromolecules* **1994,** *27*, 2685-2693.

(9) Beezer, A. E.; Loh, W.; Mitchell, J. C.; Royall, P. G.; Smith, D. O.; Tute, M. S.; Armstrong, J. K.; Chowdhry, B. Z.; Leharne, S. A., An Investigation of Dilute Aqueous Solution Behavior of Poly(oxyethylene) + Poly(oxypropylene) + Poly(oxyethylene) Block Copolymers. *Langmuir* **1994,** *10*, 4001-4006.

(10) Armstrong, J. K.; Chowdhry, B. Z.; Snowden, M. J.; Leharne, S. A., Effect of Sodium Chloride upon Micellization and Phase Separation Transitions in Aqueous Solutions of Triblock Copolymers: A High-Sensitivity Differential Scanning Calorimetry Study. *Langmuir* **1998,** *14*, 2004-2010.

(11) da Silva, R. C.; Olofsson, G.; Schillén, K.; Loh, W., Influence of Ionic Surfactants on the Aggregation of Poly(ethylene oxide)-Poly(propylene oxide)-Poly(ethylene oxide) Block Copolymers Studied by Differential Scanning and Isothermal Titration Calorimetry. *J. Phys. Chem. B* **2002,** *106*, 1239-1246.

(12) Armstrong, J.; Chowdry, B.; O'Brien, R.; Beezer, A.; Mitchell, J.; Leharne, S., Scanning Microcalorimetric Investigations of Phase Transitions in Dilute Aqueous Solutions of Poly(oxypropylene). *J. Phys. Chem.* **1995,** *99*, 4590-4598.

(13) Paterson, I.; Armstrong, J.; Chowdhry, B.; Leharne, S., Thermodynamic Model Fitting of the Calorimetric Output Obtained for Aqueous Solutions of Oxyethylene-Oxypropylene-Oxyethylene Triblock Copolymers. *Langmuir* **1997,** *12*, 2219-2226.

(14) Holtzer, A.; Holtzer, M. F., On the Use of the van't Hoff Relation in Determinations of the Enthalpy of Micelle Formation. *J. Phys. Chem.* **1974,** *78*, 1442-1443.

(15) Chiappisi, L.; Lazzara, G.; Gradzielski, M.; Milioto, S., Quantitative Description of Temperature Induced Self-Aggregation Thermograms Determined by Differential Scanning Calorimetry. *Langmuir* **2012,** *28*, 17609−17616.

(16) Wang, R.; Tang, Y.; Wang, Y., Effects of Cationic Ammonium Gemini Surfactant on Micellization of PEO-PPO-PEO Triblock Copolymers in Aqueous Solution. *Langmuir* **2014,** *30*, 1957-1968.

(17) Alexandridis, P.; Holzwarth, J. F.; Hatton, T. A., Micellization of Poly(ethylene oxide)-Poly(propylene oxide)-Poly(ethylene oxide) Triblock Copolymers in Aqueous Solutions: Thermodynamics of Copolymer Association. *Macromolecules* **1994,** *27*, 2414-2425.

(18) Janiak, J.; Bayati, S.; Galantini, L.; Pavel, N. V.; Schillén, K., Nanoparticles with a Bicontinuous Cubic Internal Structure Formed by Cationic and Non-Ionic Surfactants and an Anionic Polyelectrolyte. *Langmuir* **2012,** *28*, 16536−16546.

(19) Jansson, J.; Schillén, K.; Olofsson, G.; da Silva, R. C.; Loh, W., The Interaction between PEO-PPO-PEO Triblock Copolymers and Ionic Surfactants in Aqueous Solution Studied Using Light Scattering and Calorimetry. *J. Phys. Chem. B* **2004,** *108*, 82-92.

(20) Schillén, K.; Jansson, J.; Löf, D.; Costa, T., Mixed Micelles of a PEO-PPO-PEO Triblock Copolymer (P123) and a Nonionic Surfactant ($C_{12}EO_6$) in Water. A Dynamic and Static Light Scattering Study. *J. Phys. Chem. B* **2008,** *112*, 5551-5562.

(21) Jakeš, J., Regularized Positive Exponential Sum (REPES) Program–A Way of Inverting Laplace Transform Data Obtained by Dynamic Light Dcattering. *Collect. Czech. Chem. Comm.* **1995,** *60*, 1781-1797.

(22) Labrador, A.; Cerenius, Y.; Svenssson, C.; Theodor, K.; Plivelic, T., The Yellow Mini-Hutch for SAXS Experiments at MAX IV Laboratory. In *11th International Conference on Synchrotron Radiation Instrumentation*, Dumas, P. S. J., Ed. IOP Publishing Ltd: Lyon, France, 2013; p 072019.

(23) Hammersley, P.; Svensson, S. O.; Hanfland, M.; Fitch, A. N.; Hausermann, D., Two-Dimensional Detector Software: from Real Detector to Idealised Image or Two-Theta Scan. *High Pressure Res.* **1996,** *14*, 235-248.

(24) Orthaber, D.; Bergmann, A.; Glatter, O., SAXS Experiments on Absolute Scale with Kratky Systems using Water as a Secondary Standard. *J. Appl. Crystallogr.* **2000,** *22*, 218-225.

(25) Zemb, T.; Lindner, P., *Neutrons, X-rays and Light: Scattering Methods Applied to Soft Condensed Matter*. Elsevier Science B.V.: Amsterdam, 2002.

(26) Hansen, S., Simultaneous Estimation of the Form Factor and Structure Factor for Globular Particles in Small-Angle Scattering. *J. Appl. Cryst.* **2008,** *41*, 436-445.